DETAILED CHEMISTRY OF HEAVY ALKANE HYDROCARBON FUEL OXIDATION: APPLICATION TO COMBUSTION AND DETONATION OF GASEOUS AND LIQUID FUELS

V. Ya. Basevich[1], A. A. Belyaev[1], F. S. Frolov[1], S. M. Frolov[1,2], and S. N. Medvedev[1]

[1]N. N. Semenov Institute of Chemical Physics
Russian Academy of Sciences
Moscow, Russia
e-mail: smfrol@chph.ras.ru

[2]National Research Nuclear University
"Moscow Engineering Physics Institute" (NRNU MEPhI)
Moscow, Russia

With the improvement of personal computers and their growing capability of solving complex gasdynamic problems, many research groups all over the world are focused on the development of accurate detailed kinetic mechanisms (DKM) of fuel oxidation and combustion involving thousands reactive species and tens of thousands elementary reactions describing virtually the entire range of thermochemical parameters arising in the course of reactive system evolution. Nevertheless, it is still not feasible to use such DKMs in conjunction with three-dimensional gasdynamic simulations of reactive flows in complex geometries, in particular, with the processes of combustion, self-ignition, and detonation.

In the period from 2006 to 2014, the present authors developed and thoroughly tested a relatively short DKM of gas-phase oxidation and combustion of individual hydrocarbons of the alkane homological series from methane to n-hexadecane, alcohols, and aromatic hydrocarbons, supplemented with the DKM of nitrogen oxides formation and semiempirical reaction mechanism of soot formation, which allows monitoring not only the concentration of soot, but also the evolution of the soot-particle size distribution function. This mechanism allows simu-

lation of thermal decomposition, spontaneous and forced ignition, and combustion of multicomponent surrogate fuels and fuels with additives and was successfully applied for solving a number of gasdynamic problems associated with direct initiation of detonation and deflagration-to-detonation transition in gas mixtures, gas–drop suspensions and stratified two-phase systems, combustion stabilization in high-speed flow, reduction of emissions of harmful substances in piston and turbine engines, etc.

The objective of this work is to overview the capabilities of this DKM when applied to combustion, self-ignition, and detonation of heavy individual alkane hydrocarbons.

1 Detailed Reaction Mechanism

The DKM has been developed based on the well-known similarity in the phenomenology of oxidation of alkane hydrocarbons [1, 2] and on two simplifying assumptions: (*i*) low-temperature branching can be described by a group of reactions with only one addition of oxygen; and (*ii*) oxidation through isomers can be neglected because it is slower than oxidation through nonisomerized reactants. The algorithm for the automatic development of the DKM has been reported elsewhere [3]. According to the algorithm, for the development of the DKM of oxidation of hydrocarbon C_nH_{2n+2}, the basis is the mechanism of its analog in homologous series with a number n of carbon atoms that is smaller by a unit, i. e., $C_{(n-1)}H_{2(n-1)+2}$. This is related to reactants and to reactions. For example, the preceding analog for n-octane, C_8H_{18}, in the homologous series is n-heptane, C_7H_{16}. Therefore, the DKM of oxidation and combustion of C_1–C_7 can be taken as a basis for the construction of the DKM of oxidation and combustion of C_8. The C_1–C_7 DKM contains 81 species and 623 reactions [4]. To generate the DKM of n-octane oxidation and combustion, it was sufficient to add 9 new species and 140 new elementary reactions to the C_1–C_7 DKM [5]; thus, the resultant n-octane DKM included 90 species and 763 elementary reactions. Similarly, the n-hexadecane DKM encountered 162 species and 2380 reactions [6]. In the course of DKM construction, the computer program selects both new species and new reactions with their Arrhenius parameters and, using known rules [7], generates the thermo-

chemical database for the corresponding values of formation enthalpy and entropy, as well as specific heats at constant pressure.

It is well known that critical phenomena in chemical kinetics are reproduced only at a certain ratio of rates of different elementary acts. Therefore, during modeling of such phenomena, simple substitution of approximate values of governing rate constants does not always lead to the goal, i. e., there is a need for additional analysis and the selection of rate constants (this is valid in a theory-admissible range of values that do not exceed the experimental error). The appearance of the cool and blue flame during low-temperature spontaneous ignition of alkane hydrocarbons is one of the striking examples of such critical phenomena. For the above reason, it is necessary to correct the obtained DKM as applied to a limited number of reactions, i. e., reactions of hydrocarbons with hydroperoxide radicals and reactions of alkyl radical with molecular oxygen.

2 Validation

The DKM was thoroughly validated against experimental data for homogeneous mixture self-ignition, laminar flame velocity, and counterflow laminar flame structure, as well as for liquid drop self-ignition and combustion. Discussed below are some examples of DKM validation. In all cases discussed below, the same DKM was used without any modification.

2.1 Self-ignition of homogeneous mixtures

The self-ignition delay of homogeneous fuel–air mixtures was calculated using the KINET code developed by M. G. Neuhaus at N. N. Semenov Institute of Chemical Physics of the Russian Academy of Sciences (ICP). The underlying physicochemical model is based on the set of ordinary differential conservation equations for species and energy at constant pressure assumption. Several criteria for determining the self-ignition delay were used in the calculations including the criteria based on the rate of temperature raise (10^6 or 10^7 K/s) and that based on the time taken for the temperature T to rich the inflection point on the $T(t)$ curve (here, t is the time). Since all the criteria provided ignition delay values close to each other, the 10^7 K/s criterion was taken as a base-

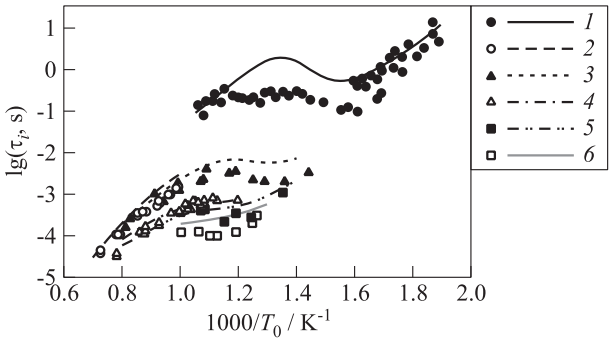

Figure 1 Ignition delay vs. initial temperature for stoichiometric n-decane–air mixtures at different initial pressures (*1* — 1.0 atm; *2* — 10; *3* — 12; *4* — 40; *5* — 50; and *6* — 80 atm) and temperatures. Curves — calculations and points — experiments [8–12]

line. In the experiments used for comparison purposes, the self-ignition delay was measured based on the records of pressure or excited species luminosity in the reaction volume.

Figure 1 compares predicted and measured ignition delays τ_i for n-decane ($C_{10}H_{22}$)–air mixtures of stoichiometric composition at different initial pressures and temperatures. Experimental data at $p_0 = 1$ atm are taken from [9], at $p_0 = 10$ and 40 atm from [11, 12], at $p_0 = 12$ and 50 atm from [8], and at $p_0 = 80$ atm from [10]. At atmospheric pressure (curve *1*), one can clearly see the domain with Negative Temperature Coefficient (NTC) of the reaction rate where ignition delays are getting longer at higher initial temperatures. The NTC domain is seen to degenerate at higher initial pressures both in calculations and in experiments. Similar to experimental findings, at low initial temperatures, self-ignition is multistage whereas at high initial temperatures, self-ignition occurs as an apparently single-stage process.

Figure 2 compares predicted (curve) and measured (points) ignition delays for stoichiometric air mixtures of alkane hydrocarbons C_nH_{2n+2} with different number of carbon atoms n ranging from $n = 3$ to 16. The values of initial temperature and pressure for this plot are taken fixed and equal to $T_0 = 787$ K and $p_0 = 15$ atm, respectively. The experimental data for these conditions are taken from the literature.

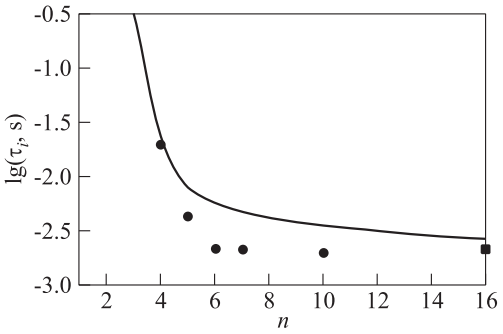

Figure 2 Ignition delay vs. the number of carbon atoms n in the alkane hydrocarbon for stoichiometric C_nH_{2n+2}–air mixtures at initial temperature $T_0 = 787$ K and initial pressure $p_0 = 15$ atm. Curve — calculations and points — experiments

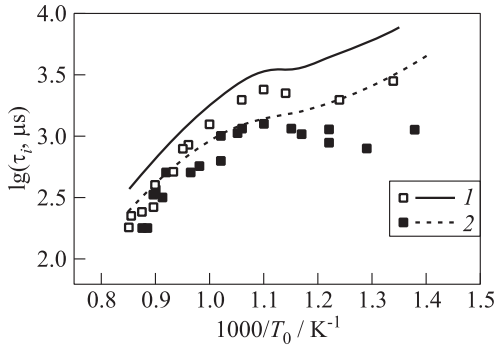

Figure 3 Ignition delay vs. initial temperature for n-dodecane–air mixtures with equivalence ratios $\Phi = 0.5$ (*1*) and 1.0 (*2*) at initial pressure $p_0 = 20$ atm. Curves — calculations and points — experiments [9, 13]

Figure 3 compares predicted (curves) and measured [9, 13] (points) ignition delays τ_i for fuel-lean and stoichiometric $C_{12}H_{26}$–air mixtures at $p_0 = 20$ atm. Clearly, the DKM provides satisfactory qualitative and quantitative predictions of the ignition delay dependences on pressure, temperature, and mixture composition. In most cases, the quantitative differences in the predicted and measured ignition delays are within the scatter of experimental data.

2.2 Laminar flame velocity

The laminar flame velocity in homogeneous fuel–air mixtures was calculated using the FLAME code developed by A. A. Belyaev and V. S. Posvianskii at ICP.

The underlying physicochemical model is based on the set of nonstationary one-dimensional partial differential equations of thermal conductivity and species reaction and diffusion at constant pressure assumption. The governing equations are solved in the code by the settling method providing the flame velocity u_n as the problem eigenvalue as well as the steady-state spatial distributions of temperature T and species concentrations. In the experiments used for comparison purposes, the laminar flame velocity is measured by different techniques related to both propagating and stabilized flames.

Figure 4 compares predicted and measured laminar flame velocities for n-heptane (C_7H_{16})–air mixtures of different equivalence ratios Φ at normal pressure and temperature.

Figure 5 compares predicted and measured laminar flame velocities for n-dodecane ($C_{12}H_{26}$)–air mixtures of different compositions at normal initial pressure and at elevated initial temperatures $T_0 = 400$ and 470 K. In all cases, a satisfactory agreement between the predicted and measured results is evident.

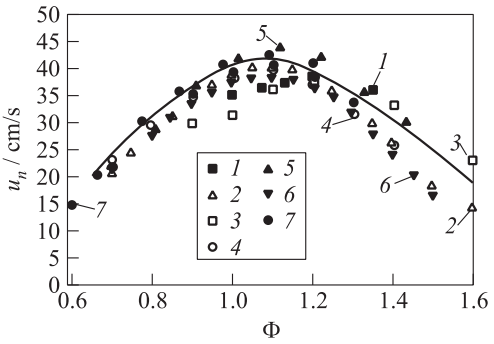

Figure 4 Predicted (curve) and measured (points) laminar flame velocities in n-heptane–air mixture vs. equivalence ratio at 1 atm and 293 K: *1* — [14]; *2* — [15]; *3* — [16]; *4* — [17]; *5* — [18]; *6* — [19]; and *7* — [20]

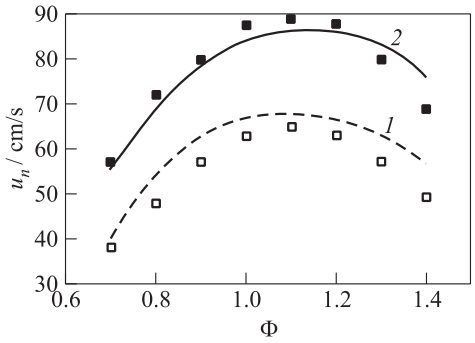

Figure 5 Predicted (curves) and measured (points) laminar flame velocities in n-dodecane–air mixture vs. equivalence ratio at 1 atm and 400 K (*1*) and 470 (*2*): points — [21]

2.3 Partially premixed laminar counterflow flames

Reported in [22] are the experimental data on spatial distributions of temperature and species concentrations in gas-phase partially premixed laminar counterflow flames of n-heptane (C_7H_{16}) and air. The n-heptane–air mixture of equivalence ratio Φ is fed through the fuel port at temperature 400 K, while pure air is fed in the opposite di-

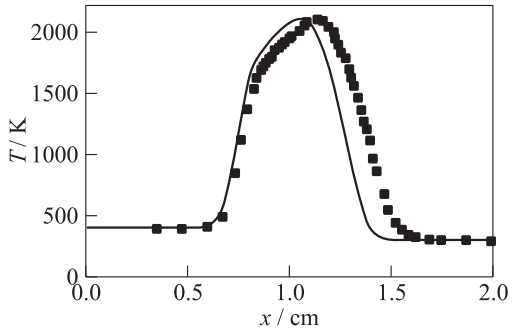

Figure 6 Predicted (curve) and measured (points) [22] temperature distributions in the partially premixed counterflow flame of n-heptane–air and air

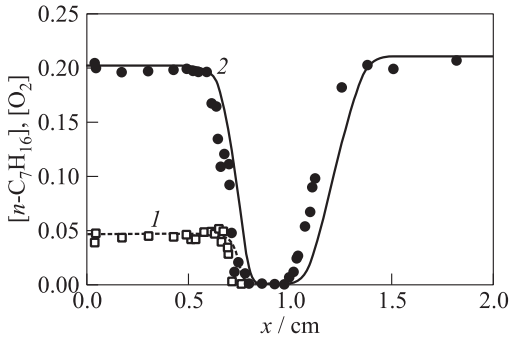

Figure 7 Predicted (curves) and measured (points) [22] distributions of n-C_7H_{16} (*1*) and O_2 (*2*) in the partially premixed counterflow flame of n-heptane–air and air

rection through the oxidizer port at temperature 300 K. The distance between the fuel and oxidizer ports is 2 cm. The experiments were conducted at atmospheric pressure. Applying the open-source CANTERA code, the flame structure was calculated at conditions reported in [22] for $\Phi = 2.5$ and global strain rate 50 s^{-1}. Figures 6 and 7 compare predicted and measured distributions of temperature (see Fig. 6) and molar fractions of n-heptane and oxygen (see Fig. 7) in the combustion zone. The agreement between the results is seen to be satisfactory.

2.4 Self-ignition and combustion of liquid drops

The self-ignition and combustion of liquid fuel drops in air was calculated using the DROP code developed by S. M. Frolov and V. S. Posvianskii at ICP. The under lying physicochemical model is based on the set of nonstationary one-dimensional (spherical symmetry) partial differential equations of energy conservation and species continuity equations in liquid and gas phases at constant pressure assumption. Applied in the code is a nonconservative finite-difference scheme and adaptive moving grid. The computational error is continuously monitored by checking balances of C and H atoms as well as energy balance at each time step. The definitions of self-ignition delay for drops were the same as for the homogeneous mixtures but all the criteria were applied to the

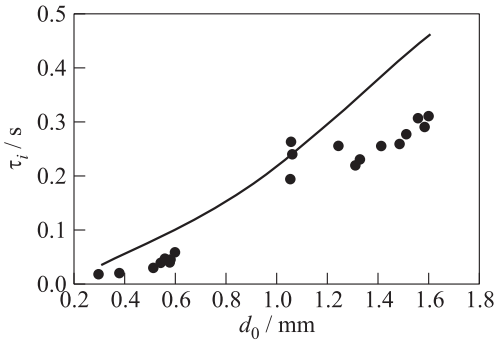

Figure 8 Predicted (curve) and measured (points) [23, 24] ignition delays of n-hexadecane drops vs. initial drop diameter at air temperature 1220 K and pressure 1 atm

maximum gas temperature due to nonuniform temperature distribution around a drop. In the experiments used for comparison purposes, the self-ignition delay was measured by the appearance of flame luminosity.

Figure 8 compares predicted (curve) and measured [23, 24] (points) dependences of the ignition delays of n-hexadecane drops in air on the initial drop diameter at initial temperature and pressure 1220 K and 1 atm, respectively. The agreement between the results can be

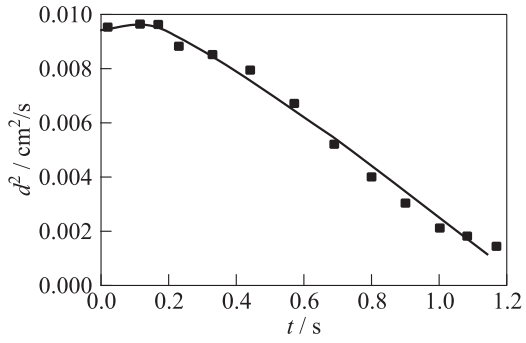

Figure 9 Predicted (curve) and measured (points) [25] squared n-decane drop diameter vs. time. Initial drop diameter 0.91 mm, initial air temperature 1093 K, and initial air pressure 1 atm

treated as satisfactory because fuel drops in the experiments were subjected to the airflow of low Reynolds number.

Figure 9 compares predicted (curve) and measured [25]) (points) time histories of the drop squared diameter at self-ignition of an n-decane drop of initial diameter 0.91 mm. At this plot, the drop self-ignites when its squared diameter starts abruptly decreasing after the slight initial growth due to thermal expansion. The rate of linear decay of the drop squared diameter is commonly referred to as the combustion constant. Clearly, as the slopes of the curve and points in Fig. 9 are the same, the predicted combustion constant corresponds well with the measured value.

3 Concluding Remarks

Thus, the DKM of n-hexadecane oxidation and combustion developed at ICP provides satisfactory predictions of self-ignition delays, laminar flame velocities, and counterflow flame structure in homogeneous fuel–air mixtures as well as self-ignition delays and combustion constants of liquid fuel drops in air for heavy alkane hydrocarbons without any need of tuning the reaction rate parameters. Despite the mechanism is rather compact, it is capable of predicting satisfactorily the multi-stage self-ignition and NTC at low-temperatures and, therefore, can be readily applied for numerical simulations of deflagration-to-detonation transition, the phenomenon which encounters both high-temperature fuel oxidation in a highly wrinkled flame front and low-temperature volumetric fuel oxidation in the preflame zones.

Acknowledgments

This work was supported by the Russian Science Foundation (grant No. 14-13-00082).

References

1. Sokolik, A. S. 1960. *Self-ignition, flame and detonation in gases*. Moscow: USSR Acad. Sci. Publ. [In Russian.]
2. Lewis, B., and G. Elbe. 1987. *Combustion, flames and explosions of gases*. Orlando: Acad. Press. 592 p.

3. Basevich, V. Ya., A. A. Belyaev, and S. M. Frolov. 2007. The mechanisms of oxidation and combustion of normal alkane hydrocarbons: The transition from C_1–C_3 to C_4H_{10}. *Russ. J. Phys. Chem. B* 2(5):477–484.
4. Basevich, V. Ya., A. A. Belyaev, V. S. Posvyanskii, and S. M. Frolov. 2010. Mechanism of the oxidation and combustion of normal paraffin hydrocarbons: Transition from C_1–C_6 to C_7H_{16}. *Russ. J. Phys. Chem. B* 4(6):985–994.
5. Basevich, V. Ya., A. A. Belyaev, S. N. Medvedev, V. S. Posvyanskii, and S. M. Frolov. 2011. Oxidation and combustion mechanisms of paraffin hydrocarbons: Transfer from C_1–C_7 to C_8H_{18}, C_9H_{20}, and $C_{10}H_{22}$. *Russ. J. Phys. Chem. B* 5(6):974–990.
6. Basevich, V. Ya., A. A. Belyaev, S. N. Medvedev, V. S. Posvyanskii, and S. M. Frolov. 2013. Mechanisms of the oxidation and combustion of normal paraffin hydrocarbons: Transition from C_1–C_{10} to C_{11}–C_{16}. *Russ. J. Phys. Chem. B* 6:161.
7. Ritter, E. R., and J. W. Bozzelli. 1991. THERM: Thermodynamic property estimation for gas phase radicals and molecules. *Int. J. Chem. Kinet.* 23(9):767–778.
8. Pfahl, U., K. Fieweger, and G. Adomeit. 1996. Self-ignition of diesel-relevant hydrocarbon–air mixtures under engine conditions. *26th Symposium (International) on Combustion Proceedings*. Pittsburgh: The Combustion Institute. 781.
9. Troshin, K. Ya. 2008. Experimental study of the ignition of n-hexane- and n-decane-based surrogate fuels. *Russ. J. Phys. Chem. B* 27:419.
10. Zhukov, V. P., V. A. Sechenov, and A. Yu. Starikovskii. 2008. Autoignition of n-decane at high pressure. *Combust. Flame* 153:130.
11. Shen, H.-P. S., J. Steinberg, J. Vanderer, *et al.* 2009. A shock tube study of the ignition of n-heptane, n-decane, n-dodecane, and n-tetradecane. *Energy Fuels* 23:2482.
12. Wang, H., S. J. Warner, A. Oehlschlaeger, *et al.* 2010. An experimental and kinetic modeling study of the autoignition of α-methylnaphthalene/air and α-methylnaphthalene/n-decane/air mixtures at elevated pressures. *Combust. Flame* 157:1976.
13. Vasu, S. S., D. F. Davidson, Z. Hong., *et al.* 2009. n-Dodecane oxidation at high pressures: Measurements of ignition delay times and OH concentration time-histories. *Proc. Combust. Inst.* 32(1):173–180.
14. Gerstein, M., O. Levine, and E. L. Wong. 1951. Flame propagation. II. The determination of fundamental burning velocities of hydrocarbons by a revised tube method. *J. Am. Chem. Soc.* 73(1):418–422.

15. Davis, S. G., and C. K. Law. 1998. Determination of and fuel structure effects on laminar flame speeds of C_1 to C_8 hydrocarbons. *Combust. Sci. Technol.* 140:427–449.
16. Kwon, O. C., M. I. Hassan, and G. M. Faeth. 2000. Flame/stretch interactions of premixed fuel–vapor/O_2/N_2 flames. *J. Propul. Power* 16:513–522.
17. Huang, Y., C. J. Sung, and J. A. Eng. 2004. Laminar flame speeds of primary reference fuels and reformer gas mixtures. *Combust. Flame* 139(3):239–251.
18. Kumar, K., J. E. Freeh, C. J. Sung, and Y. Huang. 2007. Laminar flame speeds of preheated iso-octane/O_2/N_2 and n-heptane/O_2/N_2 mixtures. *J. Propul. Power* 23:428–436.
19. Dirrenberger, P., P. A. Glaude, R. Bounaceur, H. Le Gall, A. Piras de Crus, A. A. Konnov, and F. Battin-Leclerc. 2014. Laminar burning velocity of gasolines with addition of ethanol. *Fuel* 115:162–169.
20. Nilsson, E. H. 2011. Combustion kinetics of liquid fuels. *SECOST Annual Meeting 11th Seminar Proceedings*. Lund University. 127–128.
21. Kumar, K., and C. J. Sung. 2007. Laminar flame speeds and extinction limits of preheated n-decane/O_2/N_2 and n-dodecane/O_2/N_2 mixtures. *Combust. Flame* 151:209–224.
22. Berta, P., I. K. Puri, and S. K. Aggarwal. 2006. An experimental and numerical investigation of n-heptane/air counterflow partially premixed flames and emission of NOx and PAH species. *Combust. Flame* 145:740–764.
23. Whang, J., C. Yukao, J. Ho, and S.-C. Wong. 1997. Experimental study of the ignition of single droplets under forced convection. *Combust. Flame* 110(3):366–376.
24. Yang, J., C. Yukao, J. Whang, and S.-C. Wong. 2000. Experiments on the ignition of monocomponent and bicomponent fuel droplets in convective flow. *Combust. Flame* 123(1):266–274.
25. Schnaubelt, S., O. Moriue, T. Coordes, C. Eigenbrod, and H. J. Rath Zarm. 2000. Detailed numerical simulations of the multistage self-ignition process of n-heptane, isolated droplets and their verification by comparison with microgravity experiments. *Proc. Combust. Inst.* 28:969.